International Journal of Advanced Structural Engineering, Vol. 2, No. 1, Pages 49-68, July 2010

Published online July 2010 at (http://journals.azad.ac.ir/IJASE)

CYCLIC TESTING OF STEEL CHEVRON BRACES WITH VERTICALLY SLOTTED BEAM CONNECTION

Rozlyn K. Bubela[1], Carlos E. Ventura[2] and Helmut G.L. Prion[3]
Department of Civil Engineering, University of British Columbia, Vancouver, Canada

Received 19 June 2010
Revised 10 July 2010
Accepted 15 July 2010

Experimental tests were performed to study the seismic behavior and performance of modified steel chevron braced frame systems, which incorporate a vertical slotted connection (VSC) detail between the top of the braces and the floor beam above. The VSC detail is intended to prevent vertical load transfer to the beam and limit brace forces to the compressive resistance of the members. Full-scale quasi-static cyclic tests were performed on two specimens with hollow tube braces, with one specimen having the braces filled with concrete. Both frames exhibited stable, predictable behavior under cyclic loading. The VSC detail provided free vertical movement of the brace assembly during both tests. However, its flexibility created a moderate reduction in the overall lateral stiffness of the frame. The concrete-filled tube specimen sustained higher peak loads, demonstrated greater residual strength and dissipated more energy than the hollow tube specimen due to the partial inhibition of local buckling by the concrete core. It was found that the VSC chevron braced frame system is a suitable concept for use in buildings in high-risk seismic zones.

Keywords: chevron braces, slotted beam connection, cyclic tests, energy dissipation

1. Introduction

The steel concentrically braced frame (CBF) is a common lateral load resisting system in high-risk seismic areas because of its cost-effectiveness, ease of construction and high stiffness to

[1] Former Graduate Student
[2] Professor
[3] Associate Professor

Correspondence to: Dr. Carlos E. Ventura, Department of Civil Engineering, University of British Columbia, 6250 Applied Science Lane, Vancouver, BC., Canada, E-mail: ventura@civil.ubc.ca

control the drift under wind loading and during moderate earthquakes. During very severe earthquake-induced shaking, however, CBFs may experience brittle failures at the connections or otherwise result in a slack system when braces yield, leading to a whipping effect with large accelerations. CBFs are frequently used in low-, medium- and high-rise construction and can be designed in a number of different bracing configurations, including chevron bracing. Chevron braced frames consist of two braces forming an inverted V-shape, which meet the underside of the upper storey floor beam at mid-span. When comparing different concentric bracing alternatives, chevron braces are often the most economical in terms of fabrication and erection costs versus structural effectiveness (Tremblay and Robert, 2000), and the most accommodating in terms of flexibility for locating door and window openings.

However, there are inherent drawbacks to the conventional chevron braced frame system when used in seismic design. Under moderate load conditions, the system will remain elastic and the compression and tension legs carry equal loads. Under more severe lateral load conditions, however, the compression brace in the system will buckle, thus reaching its limiting capacity or even experiencing significant loss of member strength and stiffness at larger displacements. Since the tension brace at that stage will likely still be in the elastic range, it will continue to attract more axial load and thus create a vertical load imbalance in the bracing system. This will result in a net vertical force transfer to the floor beam above, which may cause plastic hinge formation in the beam and thus compromise the gravity load resisting system of the building (Figure 1).

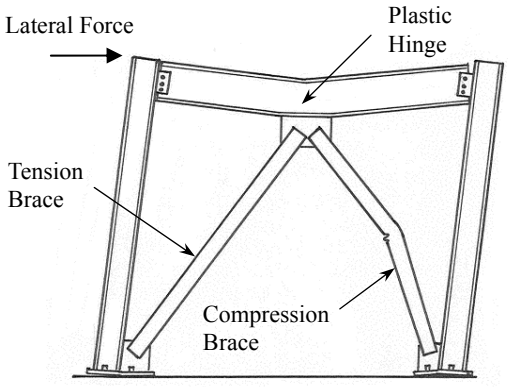

Figure 1. Conventional chevron braced frame collapse mechanism

Poor performance of chevron systems in past earthquakes and as observed in laboratory testing has lead to strict design rules limiting the use of chevron braced frames in seismic design. The current Canadian Standard for Limit States Design of Steel Structures, CAN/CSA-S16.1-94 (Canadian Standard Association, 1994), classifies the chevron brace system as a concentrically braced frame with nominal ductility (NDBF), and assigns this category of lateral load resisting systems a force modification factor of 2. This limitation is largely due to the susceptibility of

chevron brace systems to cause damage to the beam, which constitutes an important element of the gravity load resisting system of the structure. There is also a limitation on the number of storeys in buildings with chevron braced frames, based on studies demonstrating declining performance with increasing overall building height (Tremblay and Robert, 2000).

An important factor governing the design of CBFs is the capacity design philosophy that has been adopted by the Canadian code since 1989. In compliance with the principle of capacity design, the code requires that end connections of braces be designed for the full tensile capacity of the selected brace element (i.e. A_gF_y, where A_g is the gross cross-sectional area and F_y is the yield strength). In many cases, this connection force is much larger than the design force of the member, as concentric brace selection is typically based on the compression capacity of the member. This has significant implications on the cost of a structure in terms of increased material and labor costs for the structural steel system, as well as increased foundation sizes (Rezai et al., 2000).

These are significant drawbacks associated with CBF systems, which prompted further research into the complex inelastic behavior of chevron braced frames. A number of key elements have been identified in determining the level of performance of CBFs, both from observations made in laboratory testing as well as damage assessments following major seismic events. In all configurations that utilize brace elements in both tension and compression, brace buckling behavior is a key point of interest.. For conventional chevron braced frames in particular, consideration must be given to the beam design at the convergence of the brace members. The protection of the beam in chevron bracing systems has thus become a key focus of research efforts, and various design concepts for the beam have been proposed (Remennikov and Walpole, 1998 and Tremblay and Robert, 2000).

In response to the need for cost-effective design alternatives in the British Columbia (BC) region, a modified chevron braced frame concept was proposed, aimed to mitigate problems associated with conventional chevron systems. The innovative detail in the modified system incorporates a vertically slotted connection (VSC) at the junction between the inverted V-braces and the beam (Figure 2), designed to restrict vertical load transfer to the floor beam above and limit brace forces to the compression capacity of the brace members. The system was designed by Fast & Epp Consulting Engineers of Vancouver, BC and used in an industrial building in the BC Lower Mainland region.

Although the design concept was deemed valid and showed promise in reducing the earthquake demand on the structure, verification was needed to assure that no jamming of the slotted connection occurs when the braces buckle out of plane. Confirmation was also needed that plastic hinges form in the brace gussets as intended in the design. Furthermore, it was of interest to

determine the actual load-displacement behavior of the system and to assess the difference in behavior when tubular braces are filled with concrete versus leaving them empty. For these reasons, a prototype VSC chevron braced frame was designed for further testing and investigation.

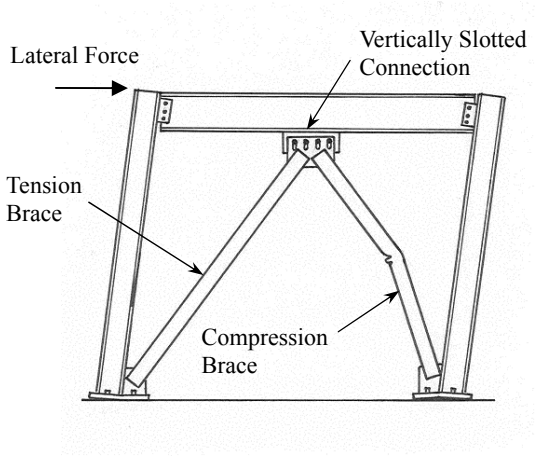

Figure 2. Vertical slotted connection chevron braced frame inelastic response

A research program was initiated to investigate the behavior of the proposed system under quasi-static cyclic loading conditions, and to assess the suitability of the VSC chevron brace system as a lateral load resisting system for high-risk seismic zones (Bubela, 2003). The focus of this paper will be the experimental testing on two full-scale specimens subjected to quasi-static cyclic loading and the interpretation of the test results.

2. Experimental Program

Full-scale tests were conducted on two VSC chevron brace specimens to study their response to quasi-static cyclic loading conditions and their energy dissipation capacity. The first specimen was tested with unfilled square hollow structural section (HSS) tube braces. For the second specimen, the HSS tube braces were filled with concrete. Material testing was also performed on samples of all steel members that were part of the chevron bracing testing assembly; this included the square HSS tube used for the brace members and two sizes of gusset plate used for the top and bottom brace-to-beam connections. All experimental testing was conducted in the Civil Engineering Structures Laboratory at the University of British Columbia.

2.1. Material Testing

Two types of standard tests were performed on the material samples. Tension tests were done for all test coupons to determine general material properties, and compression tests were done for square HSS tube columns to determine buckling characteristics of the specimens.

Tension tests were conducted on test coupons according to the appropriate American Society for Testing and Materials (ASTM) standards (American Society of Testing and Materials, 2001) prior to full-scale testing of the specimens. A series of tension tests were performed on each of the following steel material samples: HSS tube wall segments, HSS tube corner segments, 12.7 mm gusset plate and 19.0 mm gusset plate. Three tests were conducted for each material sample, and results were averaged to determine the actual material properties. The determination of yield strength was done using the 0.2% strain offset method recommended by ASTM. A summary of the material test results can be found in Table 1. The general shapes of the stress-strain curves for the HSS material samples were typical for cold-formed steel sections, with relatively undefined yield points and moderate ductility. The difference in material behavior for the two types of HSS tube samples clearly showed distinct residual stress conditions in the wall and corner segments due to the cold-forming process. As one would expect, the strength of the corner segments was higher, but the behavior more brittle. For the entire tube cross-section, the average yield strength of the HSS brace was calculated to be 455 MPa, based on weighting test results according to cross-sectional area proportioning of the tube walls and corners. The flat plate material samples showed stress-strain curves characteristic of hot-rolled steel sections and all results were within an expected range of values.

Compression tests were conducted on HSS tube samples according to the standard Stub-Column Test Procedures (Galambos, 1988). The test is designed for cold-formed steel sections with relatively thin-walled plate elements and its goals are to observe the effects of local buckling and cold forming on column strength and performance. Two stub-column tests were conducted and results were averaged to determine material properties. The determination of yield strength was done using the 0.2% strain offset method. A summary of the stub-column test results can be found in Table 1. The measured yield strength for the HSS stub-columns was in good agreement with the value determined from the tension tests. The onset of local buckling in the column specimen was characterized by the point on the stress-strain curve where the load peaks followed by an immediate reduction in strength capacity. The buckled shapes were consistent on both specimens, and consisted of outward bulges on opposite tube walls, and inward bulges on the adjacent walls. There were also slight signs of a buckling pattern along the longitudinal direction of the specimen, as the buckling shapes appeared to continue, in a much less pronounced pattern, along the remainder of the column.

Table 1. Material properties for test specimens

TEST SPECIMEN			TEST RESULTS	
Specimen Number	Specified F_y (MPa)	Specified F_u (MPa)	Actual F_y (MPa)	Actual F_u (MPa)
(a) HSS Tube Wall Test Coupons				
A1	350	450-650	422	515
A2	350	450-650	423	509
A3	350	450-650	432	517
Average	- -	- -	426	513
(b) HSS Tube Corner Test Coupons				
B1	350	450-650	583	632
B2	350	450-650	597	655
B3	350	450-650	559	617
Average	- -	- -	580	634
(c) 12.7 mm Plate Test Coupons				
C1	300	450-620	362	516
C2	300	450-620	362	518
C3	300	450-620	370	517
Average	- -	- -	365	517
(d) 19.0 mm Plate Test Coupons				
D1	350	450-650	406	573
D2	350	450-650	403	570
D3	350	450-650	404	573
Average	- -	- -	405	572
(e) HSS Stub-Columns				
E1	350	450-650	457	524
E2	350	450-650	458	525
Average	- -	- -	458	524

2.2. Chevron Brace Specimen Testing

2.2.1. Test Specimens

The steel specimens were designed according to current Canadian code provisions for bracing members (Canadian Standards Association, 1994) and dimensioned to the maximum capacity of the research facility testing frame. The specimen dimensions were 3.69 m in height and 3.51 m in width, as shown in Figure 3. The brace elements were HSS square tubes (89 mm x 89 mm x 4.8 mm) with specified yield strength of 350 MPa. The braces were slotted at the ends and welded to gusset plates to facilitate a bolted connection to the frame. At the bottom of the assembly, 12.7 mm thick gusset plates were welded to base plates with bolt-hole patterns to match the permanent testing frame. A 19.0 mm thick gusset plate with three bolt-holes was attached at the top of the braces. All the gusset plates were detailed such that a straight-line plastic hinge could form

perpendicular to the brace axis. The top brace gusset plate was positioned between two beam connection plates with vertically slotted holes. Three bolts connecting the brace gusset plate and the outer beam connection plates were fastened "finger tight" to transfer lateral loads, while permitting vertical movement along the slotted holes. The floor beam above the braces consisted of a W200x86 wide-flange member connected to two pin-ended column members below. Because of geometric limitations of the reaction frame, the height of the pin-ended columns was less than the height of the braces, but these columns were dimensioned as to permit a free lateral displacement of the top beam and to carry their share of vertical load at the same time. Two prototype brace specimens were fabricated using common fabrication techniques and tolerances. The first specimen was tested with the braces left as hollow tubes, while the brace members of the second specimen were filled with concrete. The concrete used to fill the tubes had a 28-day strength of approximately 30 MPa. No effort was made to achieve a particular concrete strength, as previous research has found that a variation of the concrete strength in the 28 to 55 MPa range would not have a significant effect on the results (Liu and Goal, 1988).

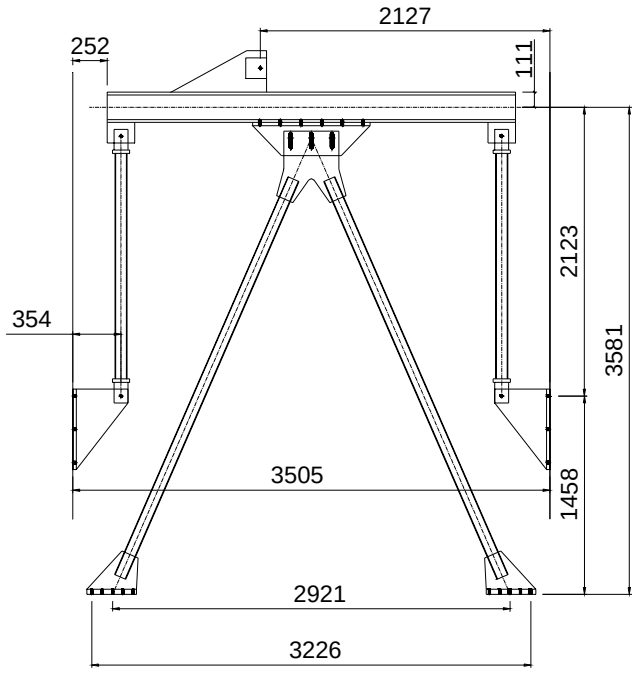

Note: Dimensions in mm.

Figure 3. Test specimen design details

2.2.2. Test Equipment and Instrumentation

The testing was done with the specimen mounted in a heavy steel reaction frame, large enough to accommodate a single-bay braced frame with realistic storey height and bay width. The testing frame was anchored to the laboratory strong floor and was stiff enough to prevent any interaction

with the forced response of the specimen being tested. Each specimen was bolted at the brace base plates to the permanent testing frame, as shown in Figure 4. The lateral load was applied to the upper floor beam by the hydraulic actuator, which had a capacity of 450 kN and a stroke of ±300 mm. The actuator displacement was controlled by an MTS servo-controller and the appropriate time versus position signals were provided by an analog function generator. Lateral support brackets with rollers were mounted on the permanent testing frame to prevent out-of-plane movements of the floor beam. Whitewashing the steel surfaces prior to testing facilitated visual observation of the yield zones.

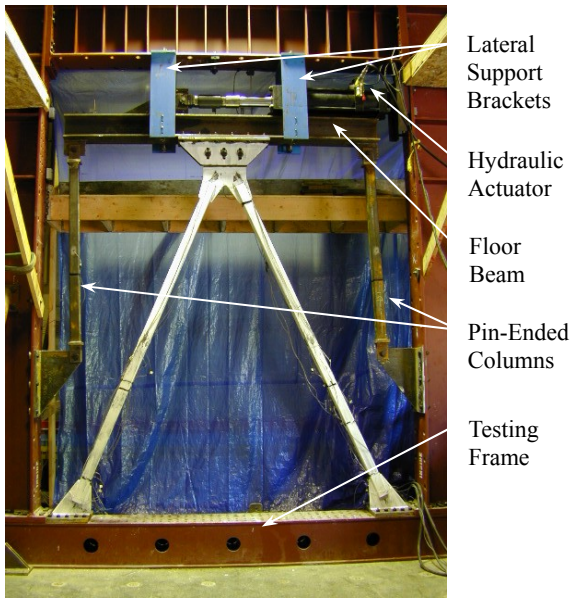

Figure 4. Test specimen set-up

Considering the small number of specimens being tested, extensive instrumentation was utilized to monitor all aspects of the specimens' behavior, which would help in the interpretation of results and enable reconstruction of events during testing. A schematic depiction of the location of instruments on the test specimen is shown in Figure 5, and a description of all instrumentation is given in Table 2. A load cell was integrated with the hydraulic actuator and both column posts were strain gauged and calibrated to measure axial loads. Displacement transducers (LVDTs and string potentiometers) were placed at various locations to measure horizontal, vertical and differential (between brace gusset plate and beam connection plate) movements of the test specimen. A number of strain gauges were mounted on the specimen to collect localized response data, and also to verify other instrument measurements. All instrument data channels were connected to a central 40-channel data acquisition system, which was in turn connected to a computer for data collection. The data was recorded at a frequency of 10 Hz.

A supplemental motion capture system was employed for Test 2. The Visualeyez™ system (Phoenix Technologies Inc., 2001) is an active-optical real-time motion tracking system that can collect three-dimensional coordinates for instrumented objects in motion. The instrumentation system included one Visualeyez™ tracker, 32 light emitting diode (LED) markers, one 64-channel target control module (TCM) used to activate and control the LED markers, and one wireless transmission system (transmitter and receiver) to send signals between the TCM and tracker. All data collected from the tracker were sent to a computer with the VZSoft™ Graphical User Interface software to view, edit and export the data.

Table 2. Test instrumentation set-up

Channel	Measured Quantity	Instrumentation
1	actuator load	load cell
2	actuator stroke	displacement transducer
3	frame lateral displacement	string potentiometer
4	beam vertical displacement	LVDT
5	slotted connection movement	LVDT
6, 7	south/north column load	2 double-rosette strain gauges
8-15	brace longitudinal strain	strain gauge
16-19	bottom gusset plate strain	strain gauge
20-31	top gusset plate strain	triple-rosette strain gauge
32	top gusset plate lateral displacement	string potentiometer

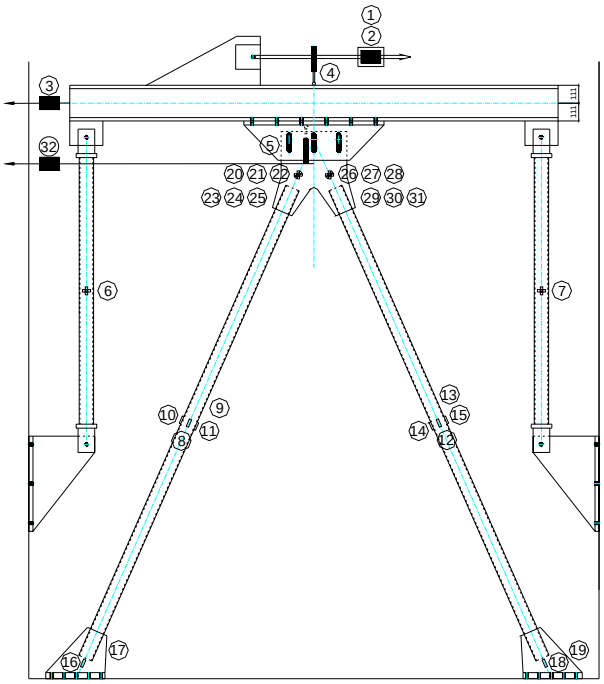

Figure 5. Test specimen instrumentation

2.2.3. Testing Program

The ATC-24 loading protocol (Applied technology Council, 1992) was chosen for the quasi-static cyclic testing of the specimens. The load history consisted of a series of stepwise increasing deformation cycles, given as multiples of the yield displacement (δ_y), as shown in Figure 6. The average loading rate varied between 14 mm/min and 28 mm/min, defined as the total displacement in a cycle divided by the cycle period. This slow, stepwise method of testing is the preferred protocol for obtaining information needed to develop design and detailing procedures and results can be considered somewhat conservative (Krawinkler, 1988). The yield displacement was chosen at the first noticeable deviation from a linear-elastic load-displacement curve. For the first specimen, this was 28 mm and, for the second specimen, 30 mm.

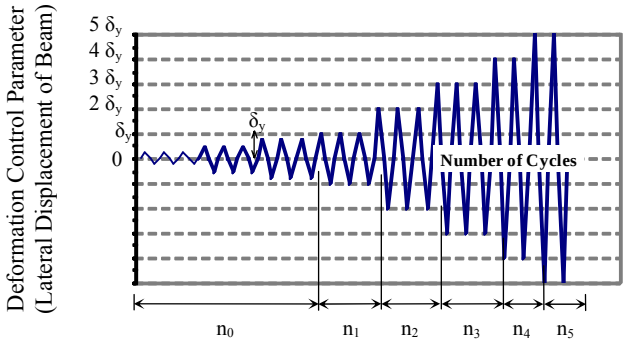

Figure 6. Nominal displacement-controlled testing pattern

Due to a sluggish response of the actuator to the control signal, it was decided to use a sinusoidal input function instead of the linear sawtooth pattern as shown in Figure 6. This was to assure that the prescribed amplitude values were reached, which meant that the loading rate varied accordingly. This compromise was deemed acceptable, as a variation in the loading rate, within acceptable limits, would not significantly influence the results. The complete sinusoidal loading protocols for Tests 1 and 2 are shown in Table 3.

3. Experimental Results

3.1. HSS Brace Specimen Testing

Testing of the first specimen continued for 12 inelastic cycles (21 cycles total) until a tension failure occurred in one of the braces (i.e. complete fracture across the brace cross-section). The maximum beam displacement was ±140 mm, approximately 3.8% storey drift. The storey drift in this case was calculated as the ratio between the lateral displacement and the height of the tested frame. The peak lateral load applied to the system was 263 kN. The hysteretic behavior of the hollow tube specimen is shown in Figure 7a.

Table 3. Test loading protocol

DISPLACEMENT CYCLE				TEST 1		TEST 2	
Step	Increment	Portion of d_y	Period (sec)	Amplitude (mm)	Number of Cycles	Amplitude (mm)	Number of Cycles
1	n_0	0.25	120	7	3	7.5	3
2	n_0	0.50	240	14	3	15	3
3	n_0	0.75	360	21	3	22.5	3
4	n_1	1.00	480	28	3	30	3
5	n_2	2.00	480	56	3	60	3
6	n_3	3.00	720	84	3	90	3
7	n_4	4.00	960	112	2	120	2
8	n_5	5.00	1200	140	2	150	2 *

* The CFT specimen was subjected to continued cyclic loading until failure, after the completion of the planned loading pattern, and experienced a total of 23 cycles at 150 mm amplitude.

3.2. CFT Brace Specimen Testing

The CFT brace specimen was still intact after completion of the proposed testing protocol. It was decided to continue cycling the specimen at the maximum displacement amplitude of ±150 mm, which was governed by limitations of the testing apparatus, until fracture and subsequent failure occurred.

Testing of the second specimen continued for 34 inelastic cycles (43 cycles total) until both braces had no further tension capacity (i.e. both braces were torn across the entire cross-section). The maximum beam displacement was ±150 mm, approximately 4.1% storey drift. The peak lateral load applied to the system was 322 kN. The hysteretic behavior of the concrete-filled tube specimen is shown in Figure 7b and the response until failure is shown in Figure 7c.

4. Discussion of Results

A number of important findings were made through observations during testing and by the comparison of results from Tests 1 and 2. A discussion of the outcomes of the experimental testing is presented here, along with the significance of these results.

4.1. Comparison to Numerical Model

A simple numerical model utilizing frame elements was used to predict the load-displacement response of the braced frame in the linear-elastic range until the onset of brace compression buckling. The critical buckling load was calculated using the Euler Formula. An effective length factor of 0.9 was assumed, according to brace and gusset plate geometry and an anticipated buckling shape. The modulus of elasticity was taken as 200,000 MPa. The critical buckling load

of the brace was estimated to be 326 kN, which corresponded to a lateral load of 259 kN on the frame.

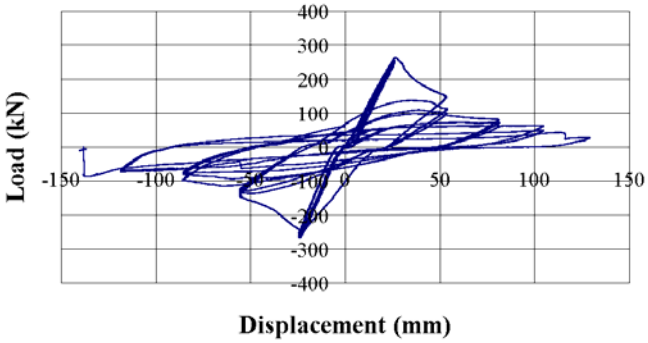

(a)

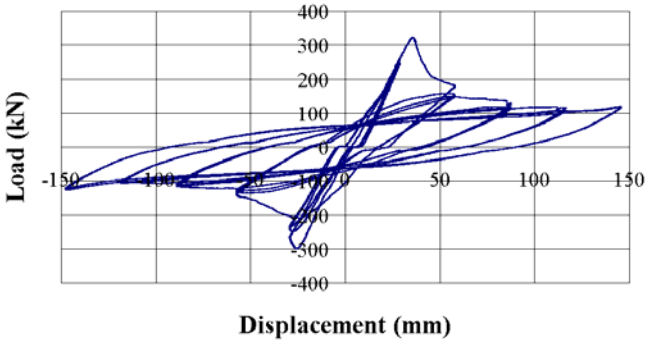

(b)

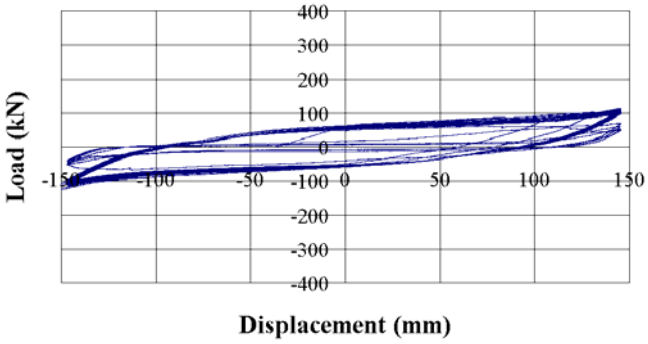

(c)

Figure 7. Load-displacement curve for cyclic loading until failure: a) Test 1, Hollow tube braces; b) Test 2, Concrete-filled tube Braces; and c) Post-Test 2, Concrete-filled tube braces

When comparing the theoretical and experimental results, good agreement of the buckling load was achieved. A major concern, however, was the large discrepancy between the frame displacement in the numerical model and the experimental frame displacement at the onset of buckling. Due to the significant difference in elastic stiffness, it became important to re-examine

the assumptions made in the theoretical model to rationalize the discrepancies between expected and observed results. In the formulation of the numerical model, the displacement was considered to be applied directly to the top of the braces, as the slotted bolted connection was assumed to offer full shear and displacement transfer from the beam to the braces. In contrast, the experimental specimen had the point of load application just above the beam, and transferred all forces and motions to the braces through the slotted bolted connection, which was considered rigid in the model.

Upon closer examination of the experimental data, evidence of a discrepancy between the displacement at the beam and the displacement at the top of the braces was observed. The differences were seen between the measured translations with the string potentiometer connected to the beam and the string potentiometer connected to the top of the braces (Figure 8). The data collected by the Visualeyez™ system during Test 2 also indicated significant differences in lateral motions at the beam level and at the top of the braces. In addition, the three-dimensional coordinates captured with the Visualeyez™ system gave further insight into the potential sources for differences between predicted and observed results. The data indicate that there was significant out-of-plane motion and rotation in the specimen at the beam and slotted connection. Thus, data measured by the string potentiometers may have included these additional motions instead of recording pure lateral deformation. A comparison between beam and brace motions measured by the string potentiometers and the Visualeyez™ system shows that the inconsistencies between the string potentiometer and Visualeyez™ data seem to diminish as the testing continued, which may be related to the out-of-plane deformations of the specimen. In the cycles when buckling first occurred, the specimen was twisting and rotating, and plastic hinges were just starting to form as out-of-plane deformations began. In the post-buckling cycles, the hinge locations were better defined and less out-of-plane motion was detected at the beam level.

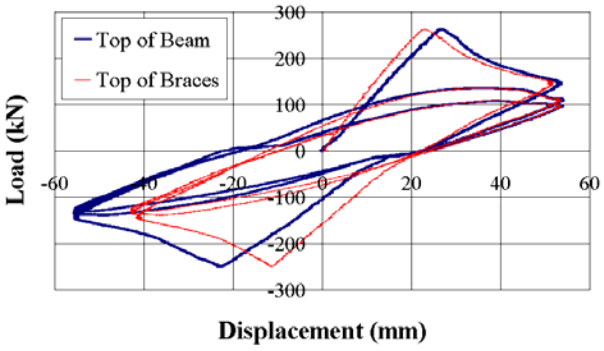

Figure 8. Comparison of displacement at top of beam and top of braces

Similar inconsistencies were seen between the theoretical prediction of yield displacement and the observed experimental values in testing done by others with bolted X-plate added damping

and stiffness (ADAS) devices between chevron braces and the supporting beam (Whittaker et al., 1988). In the ADAS device testing, it was found that the stiffness of the device was sensitive to the tightness of bolts and that the stiffness obtained was up to 35% less than predicted by assuming both plate ends to be fixed.

The discrepancy between the displacement at the beam and the displacement at the top of the braces needs to be investigated further, as these may become an important factor during rapid cycles, typical of earthquake shaking. Shake table tests can help elucidate the nature of this discrepancy and help understand better how this could affect the performance of a slotted connection during fast loading changes.

4.2. Slotted Connection Behaviour

One important goal of the experimental study was to observe the behavior of the vertical slotted connection (VSC), in anticipation of potential binding of the bolts along the slotted-holes. Distortion of the top brace gusset plate, due to plastic hinge formation after brace buckling, was expected to affect the alignment of the brace plate and beam connection plate. To address this concern, the top brace gusset plate was designed having a greater thickness than the bottom gusset plate in an attempt to minimize the effects of deformation during plastic hinge formation.

During testing, plastic deformations of the brace plates occurred directly beyond the ends of the braces at the reduced plate section. The VSC performed very well, in terms of allowing specimen vertical movement, and bolt binding was not an issue (Figure 9). The length of the slots was just sufficient to permit the travel of the bolts during the cyclic testing. At the extreme displacements during the second test, the bolts started to make contact at the ends of the slots, which is reflected in the slight increase in stiffness during large displacement cycles (Figure 7).

Figure 9. Bolt movement along vertical slotted connection

The VSC also had a significant effect on the lateral stiffness of the braced frame system. As described above, the displacements were larger than expected when compared to analytical predictions. It appears that the small gaps between the bolts and slots in the VSC detail permitted horizontal slip as well as rotation of the top brace gusset plate in the three slotted holes. When modeling a system with slotted holes, this added slippage therefore needs to be accounted for with some form of idealized translational and/or rotational springs rather than the commonly used rigid restraints. In the out-of-plane direction, the gaps between the top brace gusset plate and the slotted beam connection plates may have permitted some unexpected translation and rotation as well.

4.3. Chevron Brace Behavior

As expected, the chevron braces experienced out-of-plane buckling at loads predicted using column buckling theory. For the hollow tube brace specimen, the overall profile of the buckled compression brace had a distinct bilinear shape, due to the concentration of a plastic hinge directly at the mid-length of the brace (Figure 10a). The concrete-filled tube brace, in contrast, had a much smoother curvilinear buckled shape (Figure 10b). In the latter case, the local buckles were distributed along a greater length of the member, reducing concentrated areas of high strain, and thus maintaining the integrity of the concrete-filled tube for a greater number of cycles.

(a) (b)

Figure 10. Global buckling shape of: a) Hollow tube brace; and b) Concrete-filled tube brace

The key to the superior performance of the Test 2 specimen was the role of the concrete fill in reducing severe strains caused by local buckling in the tube walls. In testing done by others (Liu and Goel, 1988), it was found that hollow tubes exhibit early fractures in regions of plastic hinge

formation due to local buckling effects, while concrete fill works compositely with the steel tubes, resulting in more ductile behavior and better energy dissipation characteristics. These findings were also reflected in the results of the VSC chevron brace tests. Local buckling was concentrated in a central location in the hollow tube braces, which can be seen quite clearly by the pronounced indentation on one face of the tube wall, while adjacent faces buckled outward (Figure 11a). On the other hand, the local buckling pattern observed on the concrete-filled tube braces stretched over a longer region along the mid-length of the tubes, and only consisted of outward buckles, since inward buckling was resisted by the concrete fill (Figure 11b).

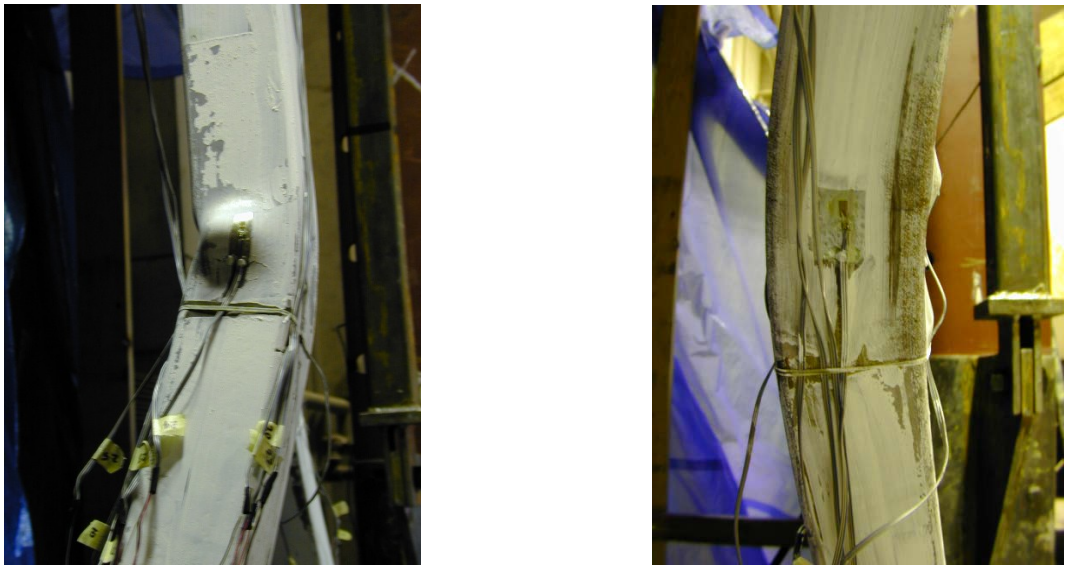

(a) (b)

Figure 11. Local buckling pattern for: a) Hollow tube brace; and b) Concrete-filled tube brace

The fracture pattern for each of the two steel tube systems was quite distinct. For the hollow tube braces, cracks were concentrated at the corners of the tube walls at locations of high residual stresses and intense strain hardening (Figure 12a). The concrete-filled tube braces maintained their integrity at the corners for a much larger number of loading cycles, and when fracture did occur, the cracks appeared to form across the entire face of the tube wall (Figure 12b). Thus, the controlling of local buckling effects in the tube walls clearly determined the progressive state of failure for the two brace specimens.

4.4. Hysteretic Behaviour

The overall ductility of the braced frame was low, in terms of the structure's ability to withstand considerable deformations without a substantial loss of strength. This was not unexpected; however, as bracing systems with compression buckling elements typically suffer a significant drop in strength and stiffness following the peak storey shear. However, the test specimen did

continue to carry a portion of its initial load capacity for a significant number of inelastic load reversal cycles before failure, indicating that there was some ductility in the brace elements.

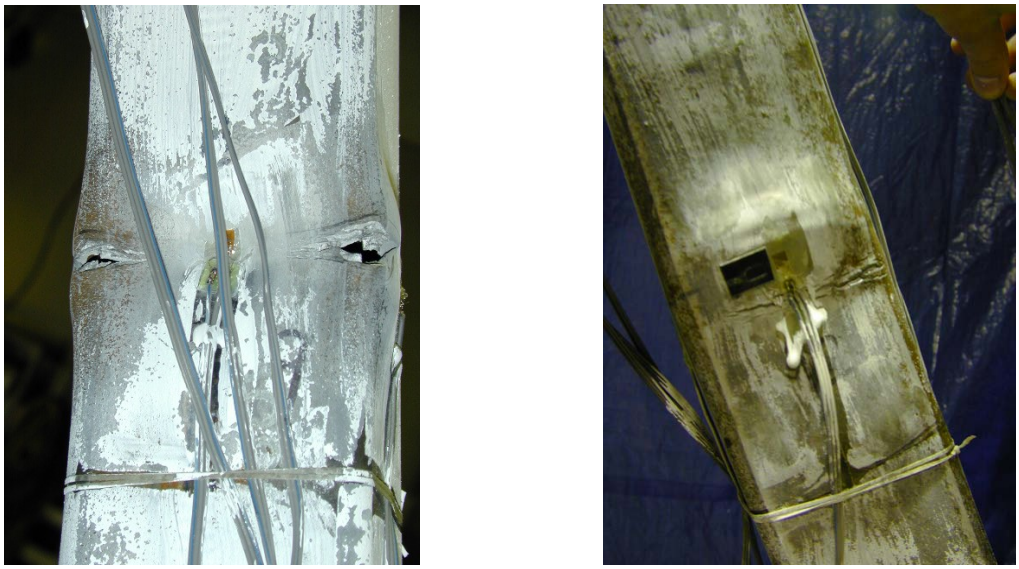

(a) (b)

Figure 12. Crack formation for: a) Hollow tube brace; and b) Concrete-filled tube brace

The strength degradation of the specimen occurred immediately following buckling of the compression brace in the system. The storey shear carried by the frame at twice the yield displacement (2 δ_y) was reduced to about 55% of the peak lateral capacity of the system at first yielding (δ_y). At three times the yield displacement (3 δ_y), the storey shear was approximately 35% of the peak lateral capacity. For the hollow tube brace specimen, at the National Building Code of Canada [14] storey drift limit of 2%, the frame capacity was about 95 kN at the first cycle of loading and 80 kN for the two subsequent displacement cycles. For the concrete-filled tube specimen, at 2% storey drift, the frame capacity was about 130 kN at the first cycle of loading and 110 kN for the two subsequent displacement cycles.

The stiffness of the specimen changed significantly after buckling of each of the brace members, which lead to the somewhat pinched hysteresis loop that is characteristic of tension-compression bracing systems. The stiffness of the frame was reduced to about 40% of its initial value in the second inelastic cycle (following buckling), and the load-displacement curve exhibited a long yield plateau region for deformations beyond the yield displacement (δ_y) at later stages of testing. This implies that once an earthquake pulse large enough to induce brace buckling occurs, it becomes questionable as to whether or not the residual stiffness of the frame will be sufficient to keep the lateral displacement of the structure within code drift limitations for the entire duration of the shaking.

Although the ductility of the system (as defined above) was low, the specimens endured a large number of inelastic load reversal cycles before fracture and ultimate failure. Therefore, the energy dissipation capacity came from the specimen's ability to undergo many displacement cycles during testing. The concrete-filled tube braces performed very well because, as local buckling effects were minimized, the number of cycles before fracture was extended, as was the service life of the brace. Due to displacement limitations of the testing apparatus, the maximum displacement amplitude of the cycles was ±150 mm (5 δ_y).

The hysteresis loops did not show much degradation when displacements remained constant for a number of cycles. This stable response for repeated cycles demonstrates the capacity of the frame to dissipate energy without rapid deterioration of the ductile brace fuse element. The energy dissipated in a cycle of testing is equal to the area under the load-displacement curve for the cycle. For the hollow tube brace specimen, the total energy dissipated was equal to 106 kJ. The amount of energy dissipated by the concrete-filled tube brace specimen was much larger than the hollow tube brace specimen, and totalled 626 kJ.

5. Conclusions

The main conclusions from this study are:

1. The chevron braces were the sole energy dissipation elements in the braced frame system during cyclic testing. Brace yielding occurred in the form of out-of-plane buckling and plastic hinge formation at the gusset plates at the ends of the braces and at the mid-span of the braces.

2. The VSC detail allowed unrestricted vertical movement of the braces throughout the entire loading history of the frame. The length of travel in the slots was just sufficient to accommodate the full range of brace vertical deformations, as the VSC bolts did not show signs of bearing on the slots until the final stages of testing. No signs of jamming between the gusset plates in the slotted connection were evident.

3. The load-displacement curves for both specimens showed the typical characteristics of tension-compression systems, where the brace elements are subjected to compression buckling. The experimental values for the peak lateral load were within 2% of the analytical estimates. However, the measured yield displacements were approximately 165% (16 mm) greater than the predicted values. The primary reason for this discrepancy is believed to result from deformations in the connections, especially the slotted connection. It can be concluded that reasonable estimates of the yield load can be expected. In the calculation of displacements, caution is advised and allowance must be made to accommodate connection flexibilities.

4. The presence of the VSC detail created a moderate reduction in the overall lateral stiffness of the braced frame system. The added flexibility in the VSC detail can be attributed to factors such as lateral slip in the slotted bolted connection, rotation in the slotted bolted connection and out-of-plane movement of the braces between the slotted beam connection plates.

5. The concrete-filled tube (CFT) specimen sustained higher peak loads and exhibited superior residual strength throughout testing when compared to the hollow tube (HSS) specimen. The degree of strength and stiffness degradation was also less severe in the CFT specimen than in the HSS specimen.

6. The deformed shape for the buckled HSS braces was distinctly bilinear, while the CFT braces showed a more curvilinear buckling shape. This was due to the degree of concentration of local buckling in the braces, as the CFT specimen distributed the effects of local buckling over a long region of the member at mid-span, while, in contrast, the HSS braces were subjected to severe local buckling in a concentrated region at the mid-span of the member. Premature fracture of the HSS tube walls at this location lead to cracking and eventual tensile failure of the brace cross-section.

7. The CFT specimen was able to resist a much larger number of inelastic cycles before fracture and failure than the HSS specimen. Almost six times more energy was dissipated in the CFT system due to the higher residual strength of braces and a greater number of effective load reversal cycles.

8. The steel VSC chevron braced frame has been shown to exhibit stable, predictable behavior under cyclic loading and is a viable concept for lateral load resisting systems in framed structures. Due to the economy and ease of construction of the system, as well as the favorable performance under cyclic loading, it is recommended that the VSC system would be suitable for use in buildings in high-risk seismic zones.

Acknowledgements

The authors would like to acknowledge the financial support of the Steel Structures Education Foundation (SSEF) of Canada, the Natural Sciences and Engineering Research Council (NSERC) of Canada, and the Department of Civil Engineering at the University of British Columbia. In addition, the authors would like to acknowledge the contributions of the Canadian Institute of Steel Construction, Fast & Epp structural engineers of Vancouver, British Columbia, Solid Rock Steel Fabricating Company of Surrey, British Columbia, and Phoenix Technologies Incorporated of Burnaby, British Columbia.

References

American Society for Testing and Materials, ASTM (2001), "Standard test methods for tension testing of metallic materials", *Test Method E8-01, ASTM*, West Conshohocken, PA., USA.

Applied Technology Council, ATC (1992), "Guidelines for cyclic seismic testing of components of Steel structures, ATC-24", *Applied Technology Council, ATC*, Washington DC., CA., USA.

Bubela, R. (2003), "An experimental and analytical study of chevron braced frames with vertical slotted connections" *MA.Sc. Thesis,* University of British Columbia, Vancouver, BC., Canada.

Canadian Standards Association, CSA (1994), "Limit states design of steel structures", *Standard CAN/CSA-S16.1-94, CSA*, Rexdale, ON, Canada.

Galambos, T.V. (1988), "Guide to Stability Design Criteria for Metal Structures, 4th Edition", *John Wiley & Sons*, New York, NY., USA.

Krawinkler, H. (1988), "Scale effects in static and dynamic model testing of structures." *9th World Conference on Earthquake Engineering*, Tokyo-Kyoto, Japan, Vol. VIII, Pages 865-876.

Liu, Z., and Goel, S.C. (1988), "Cyclic load behavior of concrete-filled tubular braces", *ASCE Journal of Structural Engineering*, Vol. 114, No. 7, Pages 1488-1506.

National Research Council Canada, NRC (1995), "National Building Code of Canada, NBCC", *National Research Council Canada (NRC)*, Ottawa, ON., Canada.

Phoenix Technologies Inc., PTI (2001), "Visualeyez™ 3D real-time motion capture system", *Phoenix Technologies Inc. (PTI)*, Burnaby, BC., Canada.

Remennikov, A. M., and Walpole, W. R. (1998), "Seismic behavior and deterministic design procedures for steel V-braced frames", *Earthquake Spectra,* Vol. 14, No. 2, Pages 335-355.

Rezai, M., Prion, H. G. L., Tremblay, R., Bouatay, N., and Timler, P. (2000), "Seismic performance of brace fuse elements for concentrically steel braced frames", *International Workshop and Seminar on Behavior of Steel Structures in Seismic Areas*, AA Balkema, Rotterdam, UK., Pages 39-46.

Tremblay, R., and Robert, N. (2000), "Seismic design of low- and medium-rise chevron braced steel frames", *Canadian Journal of Civil Engineering*, Vol. 27, No. 6, Pages 1192-1206.

Whittaker, A., Bertero, V. V., Alonso, J., and Thompson, C. (1989), "Earthquake simulator testing of steel plate added damping and stiffness elements." *Report No. UCB/EERC-89/02*, Earthquake Engineering Research Center, University of California, Berkeley, CA. USA.